Radial flow advancement in multi-layered preform for resin transfer molding

K. S. Shin, Y. S. Song and J. R. Youn*

School of Materials Science and Engineering, Seoul National University,
Shillim-Dong, Gwanak-Gu, Seoul 151-744, Korea

Abstract

Rapid flow advancement without void formation is essential in the liquid composite molding (LCM) such as resin transfer molding (RTM) and vacuum assisted resin transfer molding (VARTM). A highly permeable layer in multi-layered preform has an important role in improvement of the flow advancement. In this study, a multi-layered preform which consists of three layers is employed. Radial flow experiment is carried out for the multi-layered preform. A new analytic model for advancement of flow front is proposed and effective permeability is defined. The effective permeability for the multi-layered preform is obtained analytically and compared with experimental results. Compaction test is performed to determine the exact fiber volume fraction of each layer in the multi-layered preform. Transverse permeability employed in modeling is measured experimentally unlike the previous studies. Accurate prediction of flow advancement is of great use for saving the processing time and enhancing product properties of the final part.

Keywords : preform, resin transfer molding, permeability, woven fabric, random mat

1. Introduction

Recently, resin transfer molding (RTM) has been popular in the aircraft components, automobile parts, and military industries because it promises cost savings and performance improvement than traditional hand lay-up method (Advani *et al.*, 1994). In the resin transfer molding, a two-part mold is made out of metallic materials. Dry fiber preform is packed into a mold cavity which is made in the shape of desired part. The mold is closed and the resin is injected into the mold where it infiltrates the fiber preform. Then, the cure cycle begins and the mold and resin are heated for the polymerization reaction. Finally, the mold is opened and the composite part is removed. The greatest benefit of RTM different from other polymer composite manufacturing techniques is the separation of molding process from the design of fiber architecture. Other benefits are production of very large and complex shape, short cycle time, low labor requirement, low equipment costs, and controllable fiber volume fraction. There are a number of variables to control, e.g., resin viscosity, injection pressure, temperature of resin and mold, degree of cure, location of gates and vent holes, and permeability of the preform. In the design and tooling of the mold, it is important to predict how the mold is filled during the injection process. Permeability is one of the most important param-

eters to understand impregnation of the preform.

Experimental measurement of the permeability has been conducted in many studies (Adams and Rebenfeld, 1987; Chae, 2004; Cho *et al.*, 2003; Endruweit *et al.*, 2002; Lai *et al.*, 1997; Parnas and Salem, 1993; Weitzenböck *et al.*, 1999). In general, two experimental measurement methods, i.e. unidirectional flow and radial flow experiments, have been utilized to measure the in-plane permeability of fiber preforms, such as woven fabric, non-woven fabric, and multi-layered preform. In the RTM process, impregnation of the resin into the preform can be described by the Darcy's law which is empirically derived as the following.

$$u = -\frac{K}{\eta}\nabla P \qquad (1)$$

where **u** is the velocity vector and **K** is the permeability tensor. It is well-known that the Darcy's law provides a very good approximation of flow behavior on a macro scale (Advani *et al.*, 1994). Many researchers have investigated the permeability of multi-layered preform from unidirectional flow experiment (Bruschke *et al.*, 1992; Calado and Advani, 1996; Diallo *et al.*, 1998; Jinlian *et al.*, 2004; Luce *et al.*, 1995; Mogavero and Advani, 1997; Seong *et al.*, 2002). They usually used a weighted average permeability which could not consider transverse permeability. However, contribution of the transverse flow cannot be neglected in the multi-layered preform. Especially, when the preform is relatively thick and the difference between in-plane permeabilities of adjacent layers is large, the trans-
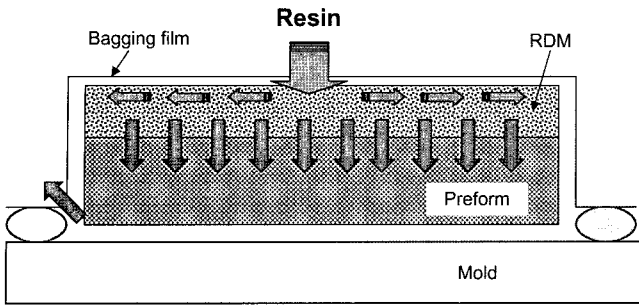
*Corresponding author: jaeryoun@snu.ac.kr

Fig. 1. Schematic diagram of VARTM.

verse flow contribution is more significant. Adams and Rebenfeld (1991) suggested a permeability model for radial flow. However, they considered only the preforms having the same porosity and used semi-permeable wall model. Chen et al. (2004) proposed an effective permeability, but could not predict exact advancement of the flow front through analytic conditions.

In multi-layered preforms, a high permeability layer plays a crucial role in the flow advancement and its permeability value greatly influences the overall in-plane permeability. Because there are limits on production of large parts and increase of fiber volume fraction in the conventional RTM, the RTM is being replaced with vacuum assisted resin transfer molding (VARTM). In the VARTM, a resin distribution medium (RDM) is placed on the preform to help the resin flow as shown in Fig. 1. The RDM makes the resin impregnation into the preform easier without voids because the moving distance of resin becomes very short (Mathur et al., 2001). Therefore, highly permeable layer like the RDM is necessary to save cost and time in the composite manufacturing process. To predict the overall permeability for multi-layered preform stack containing the layer with high in-plane permeability, contribution of the transverse flow on the entire permeability and compaction behavior of the multi-layered preform should be understood (Batch et al., 2002; Chen and Chou, 1999; Chen et al., 2001; Luo and Verpoest, 1999; Parseval et al., 1997).

In this study, advancement of flow front in multi-layered preform is predicted by using a proposed analytic model. In contrast to the previous studies, exact fiber volume fraction and height of each layer are acquired from the compaction test for the multi-layered preform and transverse permeability is measured experimentally. In order to verify the proposed analytic model, analytic results are compared with experimental ones. Effective permeability is also proposed and compared with average permeability.

2. Theory

2.1. Permeability measurement

In-plane permeability measurement is largely divided

into two methods: one is unidirectional flow experiment and the other is radial one. The unidirectional flow method can measure the individual components of permeability tensor, while the radial flow method can determine not only the principal direction but also the principal values of permeability tensor in the plane direction at the same time. In addition, the radial flow experiment avoids edge effects which are usually accompanied in the unidirectional flow experiment.

Two dimensional radial flow in porous media is described by the Darcy's law as follows.

$$v_r = -\frac{K}{\mu}\frac{\partial P}{\partial r} \qquad (2)$$

where v_r is the volume averaged fluid velocity, μ is the dynamic viscosity of the fluid, and $\partial P/\partial r$ is the pressure gradient. A mass balance in the region filled with fluid is used to obtain the radial pressure gradient. The mass balance for the case of an isotropic porous media in which the flow front has a circular shape is expressed as below.

$$2\pi r_1 v_{r1} = 2\pi r_2 v_{r2} \qquad (3)$$

where r_1 and r_2 are the two radii within the resin filled region and v_{r1} and v_{r2} are the fluid velocities in radial direction at r_1 and r_2. There are several assumptions. Firstly, all experiments are performed under constant inlet pressure. Secondly, microscopic flow, gravitational, and surface tension effects are ignored. Lastly, it is assumed that the wetted domain is fully saturated with the test fluid.

The Darcy's law and the mass balance equation are combined by using the boundary conditions of $P=P_i$ at the inlet and $P=0$ at the flow front to obtain the following equation.

$$\frac{\partial P}{\partial r} = -\frac{P_i}{r\ln(R_f/r_o)} \qquad (4)$$

where R_f is the radius of the flow front and r_o is the inlet radius. The pressure gradient varies with the reciprocal of radial position. The differential equation generated by the kinematic condition is given by

$$\frac{dR_f}{dt} = \frac{K\Delta P}{\varepsilon\mu}\frac{1}{R_f\ln(R_f/r_o)} \qquad (5)$$

where ε is the porosity of the preform, and ΔP is the pressure difference between P_f at the flow front and P_i at the inlet.

By applying the initial condition, $R_f=r_0$ at t=0, the dimensionless solution is derived as below.

$$G(\rho_f) = (\rho_f^2(2\ln\rho_f - 1) + 1)/4 = \Phi \qquad (6)$$

$$\rho_f = R_f/r_0 \qquad (7)$$

$$\Phi = Kt\Delta P/\varepsilon\mu r_0^2 \qquad (8)$$

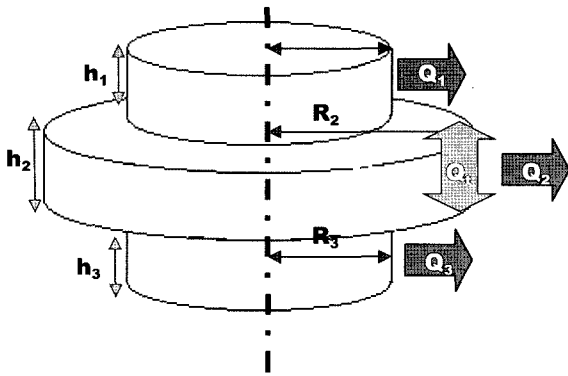where ρ_f is the dimensionless radius and Φ is the dimen-

Fig. 2. Configuration of flow advancement through multi-layered preform.

sionless time. The permeability can be obtained (Adams *et al.*, 1988; Cho *et al.*, 2003) from the experimental data of Φ vs. ρ_f by the following relation.

$$K = \frac{m\varepsilon\mu r_0^2}{\Delta P} \tag{9}$$

where m is the slope of the line obtained by the least square fitting of Φ vs. ρ_f.

2.2. Analytic model

2.2.1. Flow advancement

The multi-layered preforms selected in this study are composed of three layers and have sandwich structure as shown in Fig. 2. Adams and Rebenfeld (1991) and Bruschke *et al.* (1992) proposed analytical models for flow front advancement in the preform with two layers but didn't consider exact transverse permeability and fiber volume fraction of each layer in the multi-layered preform. On the contrary, the actual transverse permeability and fiber volume fraction obtained experimentally are taken into account in the present analytic model.

The pressure profile for radial flow is different from that of unidirectional flow. That is, the latter is assumed to be linear in the resin filled region and the former isn't. By solving the Darcy's law and the continuity equation for radial flow with proper boundary conditions, the pressure gradient with respect to radial flow direction is given by the Eq. (4).

Volumetric flow rate of each layer is obtained using the Darcy's law as follows.

$$Q_1 = Q_3 = 2\pi R_1 h_1 U_{r1} = 2\pi R_1 h_1 \left(-\frac{K_{r1}}{\mu}\frac{\partial P}{\partial r}\bigg|_{R_1}\right) = \frac{2\pi h_1 K_{r1}}{\mu}\frac{-P_i}{\ln\left(\frac{r_0}{R_1}\right)} \tag{10}$$

$$Q_2 = 2\pi R_2 h_2 U_{r2} = 2\pi R_2 h_2 \left(-\frac{K_{r2}}{\mu}\frac{\partial P}{\partial r}\bigg|_{R_2}\right) = \frac{2\pi h_2 K_{r2}}{\mu}\frac{-P_i}{\ln\left(\frac{r_0}{R_2}\right)} \tag{11}$$

$$Q_t = \frac{2\pi K_t P_i (R_1+R_2)(R_2-R_1)}{\mu(h_1+h_2)}\frac{\ln\left(\frac{R_1+R_2}{2R_2}\right)}{\ln\left(\frac{r_0}{R_2}\right)} \tag{12}$$

where Q_1, and Q_2 are the volumetric flow rate of each layer in radial flow direction, Q_t is the volumetric flow rate in the transverse flow direction, h_1 and h_2 are the thickness of each layer, U_{r1} and U_{r2} are the volume averaged fluid velocity of each layer, and R_1 and R_2 are the radius of the flow front at each layer.

Most studies on the multi-layered preform have been based on the assumption that the net flow rates between adjacent layers are equal as shown below.

$$Q_1 + Q_t = Q_2 - 2Q_t = Q_3 + Q_t \tag{13}$$

Therefore, R_1, R_2, and R_3 are calculated as follows by assuming that the volume averaged fluid velocity of each layer has reached the steady state.

$$R_1 = R_3 = \frac{t}{\varepsilon_1}\cdot\frac{Q_1+Q_t}{2\pi R_1 h_1} \tag{14}$$

$$R_2 = \frac{t}{\varepsilon_2}\cdot\frac{Q_2-2Q_t}{2\pi R_2 h_2} \tag{15}$$

By substituting Eqs. (10) to (12) to Eqs. (14) and (15), the governing equations can be obtained as the following.

$$R_1 = R_3 = \frac{t\cdot P_i}{\mu\varepsilon_1 R_1 h_1}\left\{\frac{h_1 K_{r1}}{\ln\left(\frac{r_0}{R_1}\right)} - \frac{K_t(R_1+R_2)(R_1-R_2)}{(h_1+h_2)}\frac{\ln\left(\frac{R_1+R_2}{2R_2}\right)}{\ln\left(\frac{r_0}{R_2}\right)}\right\} \tag{16}$$

$$R_2 = \frac{t\cdot P_i}{\mu\varepsilon_2 R_2 h_2}\frac{1}{\ln\left(\frac{r_0}{R_2}\right)}\left\{h_2 K_{r2} + \frac{2K_t(R_1+R_2)(R_1-R_2)}{(h_1+h_2)}\ln\left(\frac{R_1+R_2}{2R_2}\right)\right\} \tag{17}$$

where K_{r1} is the permeability of the first layer in the radial direction and K_t is the permeability in the transverse direction. There are a number of parameters in order to solve these equations. From the experimental measurements, porosities, permeabilities, and height of each layer are determined. Flow advancement with respect to time can be acquired by solving Eqs. (16) and (17) numerically.

2.2.2. Effective permeability

In this study, a new overall effective permeability is proposed in the radial flow direction. In Cartesian coordinate system, a second order permeability tensor is defined by the following the Dacry's law.

$$\begin{pmatrix} \bar{u}_x \\ \bar{u}_y \\ \bar{u}_z \end{pmatrix} = -\frac{1}{\eta}\begin{pmatrix} K_{xx} & K_{xy} & K_{xz} \\ K_{yx} & K_{yy} & K_{yz} \\ K_{zx} & K_{zy} & K_{zz} \end{pmatrix}\begin{pmatrix} \dfrac{\partial P}{\partial x} \\ \dfrac{\partial P}{\partial y} \\ \dfrac{\partial P}{\partial z} \end{pmatrix} \qquad (18)$$

For an orthotropic preform, the permeability tensor can be transformed into a symmetric matrix with zero off-diagonal terms.

$$\mathbf{K} = \begin{pmatrix} K_{xx} & 0 & 0 \\ 0 & K_{yy} & 0 \\ 0 & 0 & K_{zz} \end{pmatrix} \qquad (19)$$

The overall flow rate is expressed in the radial direction as follows.

$$Q = \frac{-2\pi H P_i \bar{K}}{\mu \ln\left(\frac{r_0}{R}\right)} \qquad (20)$$

$$\bar{R} = \frac{1}{H}\sum_{i=1}^{n} r_i h_i \qquad (21)$$

where $\bar{K}$ is the effective permeability and $\bar{R}$ is the effective radius of the flow front. According to the mass balance, the total flow rate is also given as below.

$$Q = Q_1 + Q_2 + Q_3 = 2Q_1 + Q_2 \qquad (22)$$

By substituting Eqs. (10), (11), and (20) into Eq. (22), the effective permeability can be obtained as the following.

$$\bar{K} = \frac{\ln\left(\frac{r_0}{\bar{R}}\right)}{H}\left(\frac{2h_1 K_{r1}}{\ln\left(\frac{r_0}{R_1}\right)} + \frac{h_2 K_{r2}}{\ln\left(\frac{r_0}{R_2}\right)}\right) \qquad (23)$$

3. Experiment

3.1. Materials and experimental setup

The preforms selected in this study were plain woven fabrics, glass random mats, and circular braided hybrid preforms. The plain woven fabrics included glass fiber woven fabrics, aramid fiber woven fabrics, hybrid fiber woven fabrics and carbon fiber woven fabrics. The fluid used in this study was the silicone oil (dimethyl siloxane polymer, DC 200F/100CS) supplied by Dow Corning. The silicone oil showed Newtonian behavior and the viscosity of the silicone oil was 9.7×10^{-2} Pa·s.

The mold designed for the two-dimensional radial flow experiment is schematically illustrated in Fig. 3. The radial flow was generated by injecting the fluid through a central
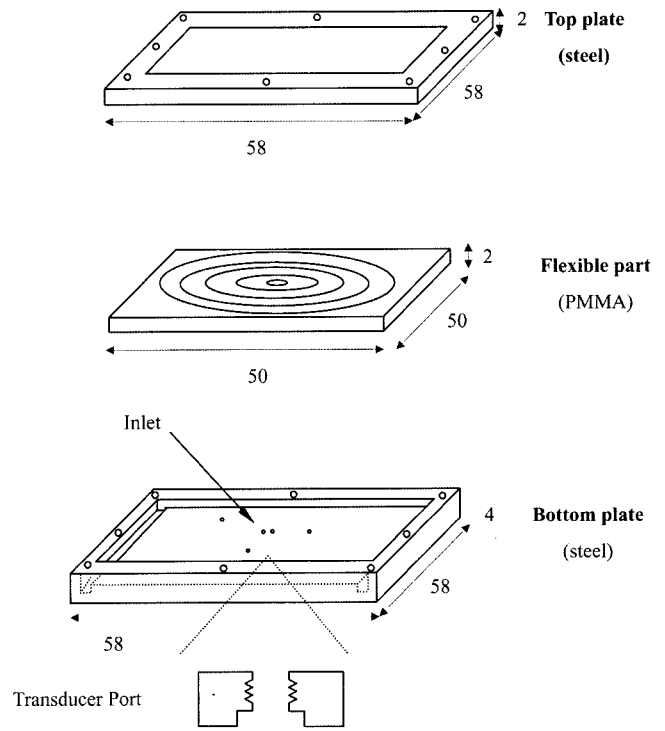

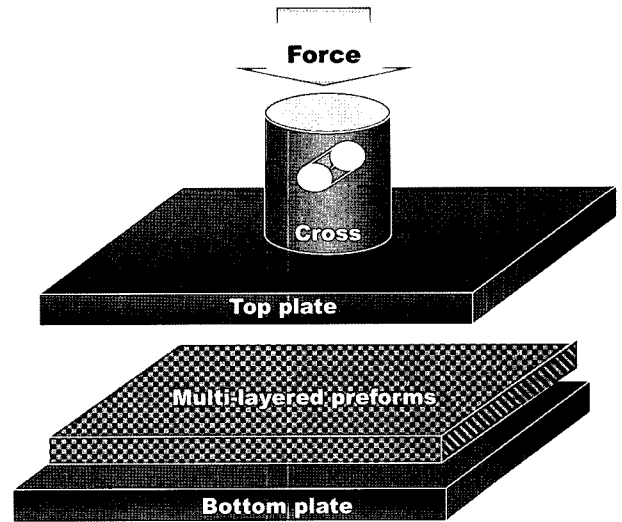Fig. 3. Schematic diagram of mold cavity used in radial flow experiment.

Fig. 4. Schematic illustration of compaction test.

gate into a 500×500 mm cavity between two parallel plates containing the reinforcing fiber structure. The upper transparent plate is made out of acrylic resin (PMMA), which enabled us to observe the mold-filling pattern visually. A digital camcorder was used to record the flow pattern.

A MTS (Material Test System) machine was used to perform compaction test for the preforms. The empirical setup is illustrated in Fig. 4. A grip for the tensile test was replaced with horizontal plates. The plates were made of

stainless steel with a rectangular shape. Upper mold was connected to a load cell of the MTS machine and lower one was placed on the flat plate. Preform layers of 80×80 mm^2 were stacked uniformly and were located between flat steel plates. The load range used was 0-20 kN and compression rate was 1 mm/min. Thickness of the fabric stack was measured with respect to the imposed load.

3.2. Permeability measurement

Permeabilities of glass fiber random mats, glass fiber plain woven fabrics, aramid fiber plain woven fabrics, and hybrid plain woven fabrics were measured by the unsaturated radial flow experiment. The resin was injected to the mold under constant low pressure. Pressure of liquid resin was measured by pressure transducers at the inlet. The permeability was measured at different fiber volume fractions by compressing the fiber preform to different heights. The multi-layered preform shown in Fig. 2 was utilized. The preform consisted of three layers. Top and bottom layers were the same preforms and the middle layer had the highest permeability among three layers. The preform had a sandwich structure. The top and bottom layers were aramid fiber plain woven fabrics and the middle layer was glass fiber plain woven fabric.

In order to obtain transverse permeability, transverse flow experiment in the gapwise direction was performed. The steady state flow rate was measured by collecting the outflow from the mold during measured time. The pressure gradient was obtained by pressure transducers after the fiber preforms were completely impregnated. The transverse permeability of the fiber preform was calculated through the Darcy's law.

4. Results and discussion

4.1. In-plane permeability

Four different homogeneous preforms and one multi-layered preform are used for radial flow experiment. The middle layer can increase the total permeability and the flow rate significantly as a highly permeable preform. From the experiment for homogeneous preforms, a glass fiber plain woven fabric is selected as the highly permeable layer.

As shown in Fig. 5, the permeability of glass fiber plain woven fabric has the largest value and that of aramid fiber plain woven fabric has the smallest value. From the standpoint of micro-structural scale, it is explained by the fact that the number of yarns per unit length of glass fiber plain woven fabric is the lowest among four different fabrics. Permeability of the multi-layered preform varies between permeabilities of glass fiber and aramid fiber plain woven fabrics. The highly permeable middle layer leads to enhancement of the total permeability. Because of the blocking effect, permeability of each preform is decreased with increase in the fiber volume fraction.
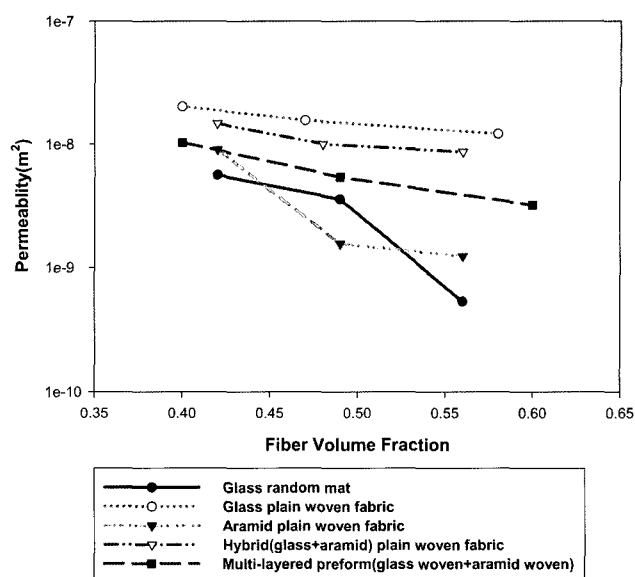

Fig. 5. Permeabilities in radial direction with respect to fiber volume fraction.

4.2. Transverse permeability

Transverse permeabilities of the glass fiber plain woven fabric, aramid fiber plain woven fabric, hybrid plain woven fabric and carbon fiber woven fabric are plotted as a function of fiber volume fraction as shown in Fig. 6 and 7. In order to study the effect of fiber volume fraction on the transverse permeability, fiber woven fabrics of the same structure are used. Figs. 6 and 7 show that the influence of the number of preforms on the permeability cannot be neglected. As the fiber volume fraction is increased, the transverse permeability is decreased. These results can be explained by the blocking effect at the interface of two adjacent fiber mats, which created tortuous flow paths. The glass fiber plain woven fabric has the highest transverse permeability because inter-fiber structure of the glass fiber woven fabric is sparser than those of the others.

4.3. Compaction behavior of the preforms

In compaction test, all the preforms were compressed to a final thickness at constant crosshead speed of 1.0 mm/min. The compression load vs. fabric preform thickness is plotted in Fig. 8, where results of multi-layered preforms and homogeneous preforms are compared. It is observed that the compacted thickness of multi-layered preform varies between those of homogeneous layers.

In resin transfer molding, after the mold is closed, the fiber preform is inevitably compressed and the exact fiber volume fraction cannot be estimated. Therefore, the exact fiber volume fraction is obtained by the experimental compaction test. The predicted fiber volume fraction is used in the analytic model for flow advancement.
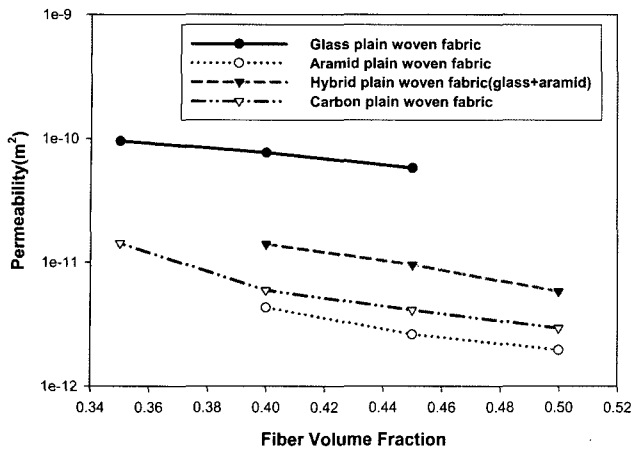
Fig. 6. Transverse permeability measured with respect to fiber volume fraction when 10 layer preform is employed.
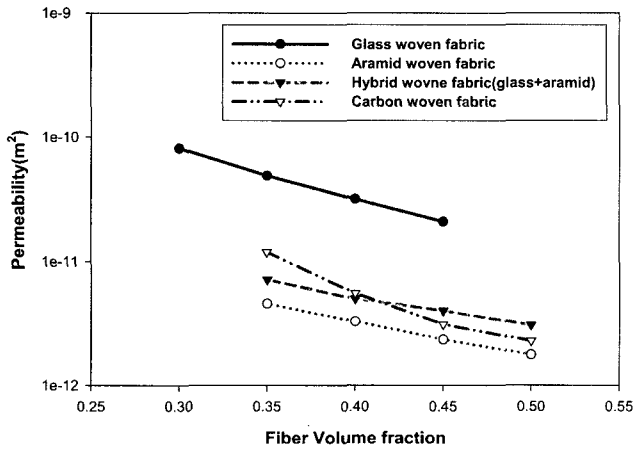

Fig. 7. Transverse permeability measured with respect to fiber volume fraction when 20 layer preform is employed.
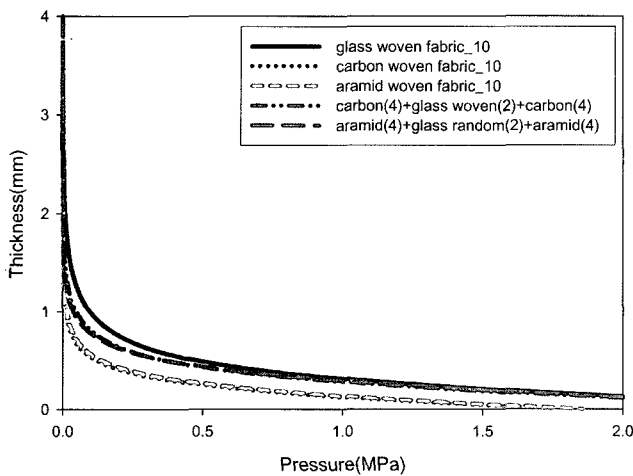

Fig. 8. Thickness versus pressure curves obtained from compaction test for homogeneous preforms and multi-layered preforms.
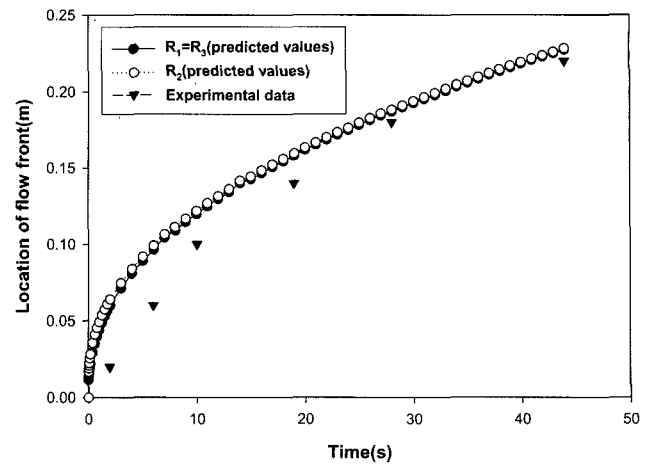

Fig. 9. Predicted and measured advancement of flow front.
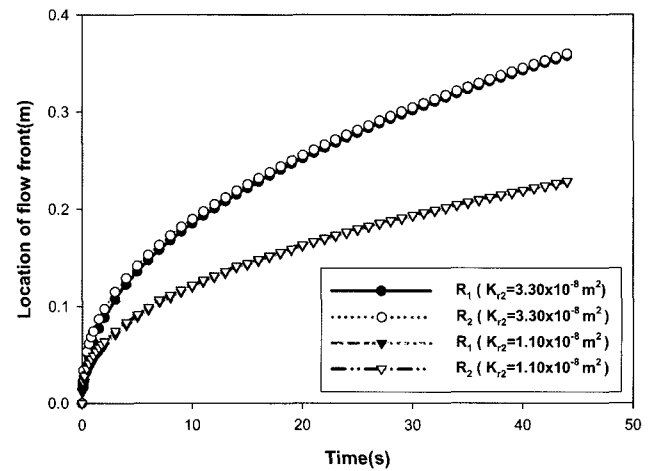

Fig. 10. Predicted flow front advancement for multi-layered preform with different radial permeability of middle layer.

4.4. Multi-layered preform with sandwich structure

Fig. 9 shows that the difference between predicted results and experimental data is decreased as time elapses. The flow front advancements obtained analytically are in good agreement with the experimental results such that the analytic model can predict the filling time precisely. The effect of permeability of the middle layer on the overall flow front advancement is shown in Fig. 10. The predicted flow front advancement through the middle layer with permeability of 3.3×10^{-8} m^2 is twice as fast as that through the middle layer with permeability of 1.1×10^{-8} m^2. Advancement of flow front for multi-layered preform with low transverse permeability is shown in Fig. 11. The difference between flow fronts becomes large due to small transverse flow across the preforms. The advancement of flow front is highly affected by the transverse flow between neighboring layers.

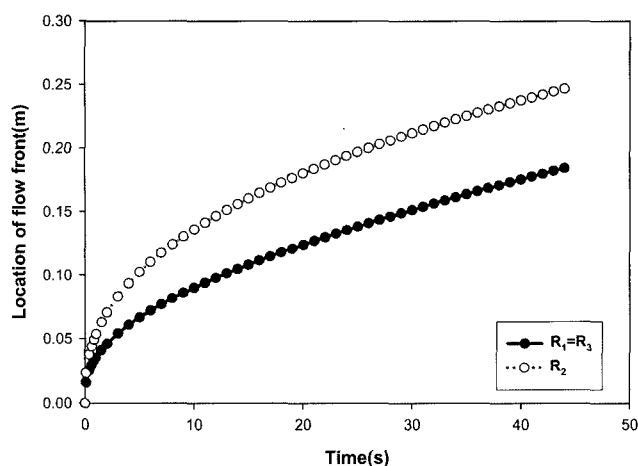In most studies, the average permeability that does not

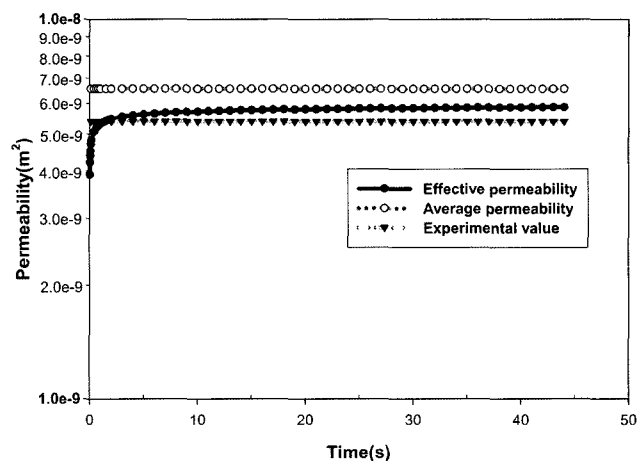**Fig. 11.** Predicted flow front advancement for multi-layered pre-form with low transverse permeability.

Fig. 12. Comparison of effective permeability, average permeability and experimental value.
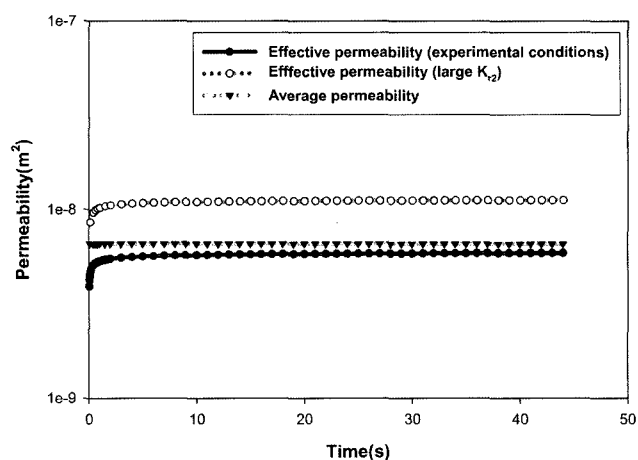

Fig. 13. Influence of high in-plane permeability of middle layer on the effective permeability.

account transverse permeability has been adopted for prediction of the radial flow. In this study, the effective permeability considering the transverse permeability is employed. In Fig. 12, the effective permeability predicted in the same condition of the experiment, the average permeability, and experimental data are compared. Because the scheme for the average permeability simply does not consider the transverse permeability, it provides much higher permeability than the experiment. It is found that the proposed effective permeability is more appropriate for predicting the overall permeability than the average permeability. Fig. 13 shows that as in-plane permeability for the middle layer is increased, the effective permeability is increased.

5. Conclusions

Most previous studies on the resin flow through multi-layered preforms have handled unidirectional flow without considering the transverse permeability or fiber volume fraction of each layer. A new analytic model for the advancement of flow front and the effective permeability of a multi-layered preform are proposed. The employed multi-layered preform has the sandwich structure composed of three layers. In order to determine the exact fiber volume fraction of each layer in the multi-layered preform, compaction test is carried out. Analytic and experimental results for flow front advancements are in good agreement. The proposed effective permeability is closer to the permeability measured experimentally than the average permeability. From the analytical modeling of flow front advancement, it is found that the transverse flow across neighboring layers plays a significant role in the entire resin flow. The sandwich preform structure employed in this study can be utilized to reduce the processing time in the RTM and VARTM.

Acknowledgements

References

Adams, K.L. and L. Rebenfeld, 1987, In-plane flow of fluids in fabrics: structure/flow characterization, *Textile Res. J.* **57**, 647.

Adams, K.L. and L. Rebenfeld, 1991, Permeability characteristics of multilayer fiber reinforcements. Part I: experimental observations, *Polym. Compos.* **12**, 179.

Adams, K.L. and L. Rebenfeld, 1991, Permeability characteristics of multilayer fiber reinforcements. Part II: theoretical model, *Polym. Compos.* **12**, 186.

Adams, K. L., W. B. Russel and L. Rebenfeld, 1988, Radial penetration of viscous liquid into a planar anisotropic porous medium, *Int. J. Multiphase Flow* **14**, 203.

Advani, S.G., M.V. Bruschke and R.S. Parnas, 1994, Flow and Rheology in Polymer Composites Manufacturing, Elsevier, Amsterdam.

Batch, G.L., S. Cumiskey and C.W. Macosko, 2002, Compaction of fiber reinforcements, *Polym. Compos.* **23**, 307.

Bruschke, M.V., T.L. Luce and S.G. Advani, 1992, Effective in-planer permeability of multi-layered RTM performs, Proceedings of the 7th Technical Conference of the American Society for Composites, University Park, PA, U.S.A., 103.

Calado, V.M.A. and S.G. Advani, 1996, Effective average permeability of multi-layer preforms in resin transfer molding, *Compos. Sci. Technol.* **56**, 519.

Chae, H.S., 2004, Out-of-plane permeability measurement of braided preform in resin transfer molding, Master Thesis, Seoul National University, Seoul.

Chen, B. and T.W. Chou, 1999, Compaction of woven-fabric preforms in liquid composite molding process: single-layer deformation, *Compos. Sci. Technol.* **59**, 1519.

Chen, B., A.H.D. Cheng and T.W. Chou, 2001, A nonlinear compaction model for fibrous performs, *Compos. Part A* **32**, 701.

Chen, Z., L. Ye and H. Liu, 2004, Effective permeabilities of multilayer fabric preforms in liquid composite moulding, *Compos. Struct.* **66**, 351.

Cho, Y.K., Y.S. Song, T.J. Kang, K. Chung and J.R. Youn, 2003, Permeability Measurement of a circular braided preform for resin transfer molding, *Fibers and Polymers* **4**, 135.

Diallo, M.L., R. Gauvin and F. Trochu, 1998, Experimental analysis and simulation of flow through multi-layer fiber reinforcements in liquid composite molding, *Polym. Compos.* **19**, 246.

Endruweit, A., T. Luthy and P. Ermanni, 2002, Investigation of the influence of textile compression of the out-of-plane permeability of a bidirectional glass fiber fabric, *Polym. Compos.* **23**, 538.

Jinlian, H., L. Yi and S. Xueming, 2004, Study on void formation in multi-layer woven fabrics, *Compos. Part A* **35**, 595.

Lai, Y.H., B. Khomami and J.L. Kardos, 1997, Accurate permeability characterization of preforms used in polymer matrix composite fabrication process, *Polym. Compos.* **18**, 368

Luce, T.L., S.G. Advani, J.G. Howard and R.S. Parnas, 1995, Permeability characterization. Part 2: flow behavior in multiple-layer performs, *Polym. Compos.* **16**, 446.

Luo, Y. and I. Verpoest, 1999, Compressibility and relaxation of a new sandwich textile preform for liquid composite molding, *Polym. Compos.* **20**, 179.

Mathur, R., D. Heider, C. Hoffmann, J.W. Gillespie, S.G. Advani and B.K. Fink, 2001, Flow front measurements and model validation in the vacuum assisted resin transfer molding process, *Polym. Compos.* **22**, 477.

Mogavero J. and S.G. Advani, 1997, Experimental investigation of flow through multi-layered performs, *Polym. Compos.* **18**, 649.

Parnas, R.S. and A.J. Salem, 1993, A comparison of the unidirectional and radial in-plane flow of fluids through woven composite reinforcements, *Polym. Compos.* **14**, 383.

Parseval, Y.D., K.M. Pillai and S.G. Advani, 1997, A simple model for the variation of permeability due to partial saturation in dual scale porous media, *Transport in Porous Media* **27**, 243.

Seong, D.G., K. Chung, T.J. Kang and J.R. Youn, 2002, A study on resin flow through a multi-layered preform in resin transfer molding, *Polym. Polym. Compos.* **10**, 493.

Weitzenböck, J.R., R.A. Shenoi and P.A. Wilson, 1999, Radial flow permeability measurement. Part A : theory, *Compos. Part A* **30**, 781.

Weitzenböck, J.R., R.A. Shenoi and P.A. Wilson, 1999, Radial flow permeability measurement. Part B: application, *Compos. Part A* **30**, 797.